

## Electron-ion relaxation time dependent signal enhancement in ultrafast double-pulse laser-induced breakdown spectroscopy

S. S. Harilal,<sup>a)</sup> P. K. Diwakar, and A. Hassanein

Center for Materials Under Extreme Environment, School of Nuclear Engineering, Purdue University, West Lafayette, Indiana 47907, USA

(Received 15 April 2013; accepted 5 July 2013; published online 22 July 2013)

We investigated the emission properties of collinear double-pulse compared to single-pulse ultrafast laser induced breakdown spectroscopy. Our results showed that the significant signal enhancement noticed in the double pulse scheme is strongly correlated to the characteristic electron-ion relaxation time and hence to the inter-pulse delays. Spectroscopic excitation temperature analysis showed that the improvement in signal enhancement is caused by the delayed pulse efficient reheating of the pre-plume. The signal enhancement is also found to be related to the upper excitation energy of the selected lines, i.e., more enhancement noticed for lines originating from higher excitation energy levels, indicating reheating is the major mechanism behind the signal improvement. © 2013 AIP Publishing LLC. [<http://dx.doi.org/10.1063/1.4816348>]

The recent advancements in fs laser technology stimulated the development of a new field called ultrafast laser-induced breakdown spectroscopy (ULIBS), or fs LIBS.<sup>1-3</sup> Even though the only difference between the conventional ns laser based LIBS and ULIBS is the difference in laser system, the mechanisms leading to energy absorption and subsequent target ablation are entirely different for both cases due to significant higher rate of energy deposition in fs laser ablation (LA). Approximate time scales of ns and fs laser energy absorption and ablation, along with various processes occurring during and after the laser pulse, are given in detail elsewhere.<sup>1,4</sup> On the other hand, ionization, sample heating, and vaporization all occur during the laser pulse in ns LA, fs laser pulses are sufficiently short that these phenomena do occur at a later time compared to the excitation pulse duration. Because of this time difference in the ablation processes, fs laser excitation results in smaller heat affected zone (HAZ), more reproducible material ablation, ablation products resembling bulk stoichiometry, and minimal elemental fractionation and matrix effects.<sup>4</sup> In fs LA, the electron impact ionization and strong electric field ionization (photo-ionization) are the major processes for free electron generation, while the Coulomb explosion (gentle ablation) and thermal vaporization (strong ablation) are the two competing mechanisms resulting in material removal and ablation.<sup>5</sup> Limited HAZ in ULIBS also prevents uncontrollable and undesirable material modification and removal as seen with longer pulse laser ablation. In the LIBS point of view, fs LA also provides lesser continuum, atomic and molecular plume, higher signal stability, and cleaner ablation in comparison with ns LA.<sup>4,6-9</sup> Moreover, fs laser filamentation can be implemented for remote LIBS analysis.<sup>10</sup>

Double-pulse (DP) or pre-pulse technique is commonly used in ns LIBS for improving the analytical accuracy of the measurements.<sup>11</sup> Double-pulse technique is also routinely used for increasing conversion efficiency of x-ray<sup>12</sup> or EUV radiation<sup>13</sup> in laser-produced plasma sources. Extensive

studies have already been carried out using various ns DP configurations (collinear, orthogonal, pre-ablation LIBS, crossed beam) as well as by varying laser parameters; specifically wavelength of irradiation.<sup>14</sup> Recent research involving ns lasers showed that shorter wavelength pre-pulsing followed by IR re-heating laser provided the highest signal enhancements.<sup>15</sup> However, the wavelength of excitation is expected to play a lesser role in ULIBS due to significantly shorter duration of the pulse compared to electron-to-ion energy transfer and heat conduction times which are typically a few ps.<sup>6</sup> Recent results employing fs DP-LA showed very promising results in the fields of LIBS<sup>16</sup> and material modification.<sup>17</sup> In this letter, we report that the signal enhancements in DP ULIBS are highly dependent on the upper excitation energy levels of the emission lines and is strongly influenced by electron-ion relaxation time.

The schematic of the experimental scheme used for the present studies is given in Figure 1. Briefly, a 10 Hz, 800 nm, 100 fs Ti: Sapphire laser (Amplitude Technology) was used for constructing a Michelson interferometer. A 50:50 beam splitter was employed for dividing the beam into two. Two right-angled prisms were used for retro-reflecting the beams in both arms of the interferometer. Since the fs laser pulses are inherently broadband, the beam is susceptible to group velocity dispersion (GVD) when it passes through a medium like right-angled prism. However, GVD and associated group delay dispersion (GDD) are important considerations for pulses with width  $\leq 50$  fs, but less significant for pulses  $> 100$  fs. The right-angled prism used in one of the arms of the interferometer was positioned on a high precision micrometer translator which allowed to introduce an optical delay up to 50 ps with a precision of  $\sim 66$  fs. Both beams approach the brass target in air collinearly and focusing was made using a plano-convex lens with  $f = 10$  cm with an approximate spot radius of  $50 \mu\text{m}$ . The laser fluence used in the experiment was in the range  $2.5\text{--}12.7 \text{ J/cm}^2$ . For the single pulse experiment, one of the arms is blocked using a laser beam dump. The plasma emission was collected using an off-axis parabolic mirror and focused onto a fiber tip. The

<sup>a)</sup>hari@purdue.edu

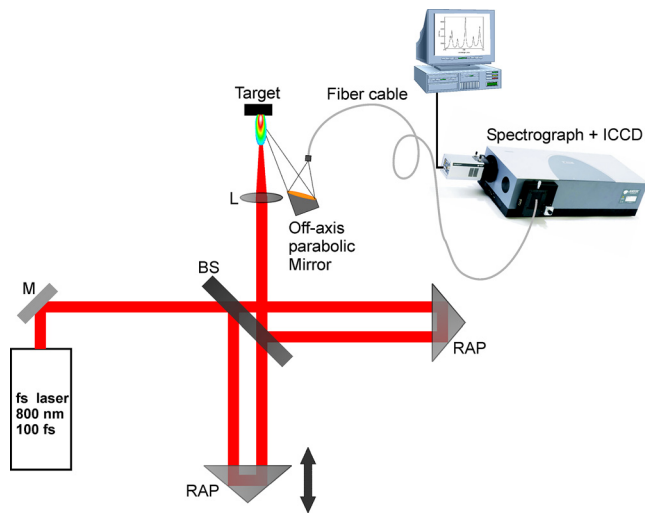


FIG. 1. Schematic of ULIBS using fs laser beams. A 10 Hz, 100 fs laser beam was split using a 50/50 beam splitter (BS) for constructing a Michelson's interferometer. Right-angle prisms (RAP) were used for retro-reflecting the beams. The right-angle prism in one of the arms of interferometer was positioned in a high-precision translator for varying the delays between two pulses reaching the target (M, mirror; and L, lens).

fiber was coupled to a three-grating 0.75 m Andor Shamrock spectrograph that was equipped with an intensified charged coupled device (ICCD, Andor iStar) for dispersed light analysis.

Figure 2 displays the emission spectra from ultrafast single pulse (SP) LIBS and DP-LIBS from brass plasma. The spectra were recorded with a gate width of  $1 \mu\text{s}$  with a delay of 0 ps for both SP and DP measurements while a 20 ps inter-pulse delay was used for DP measurements. The prominent lines seen in the spectra include 465.11, 510.55, 515.32, 521.82 nm Cu I and 468.01, 472.21, 481.05 nm Zn I transitions. Compared to ns plasma, the fs plasma emission spectra are less influenced by ambient environment indicated by reduced broadening of lines and reduced continuum emission.<sup>18</sup> Reduced continuum emission shows a good promise for improving the limit of detection for major and trace

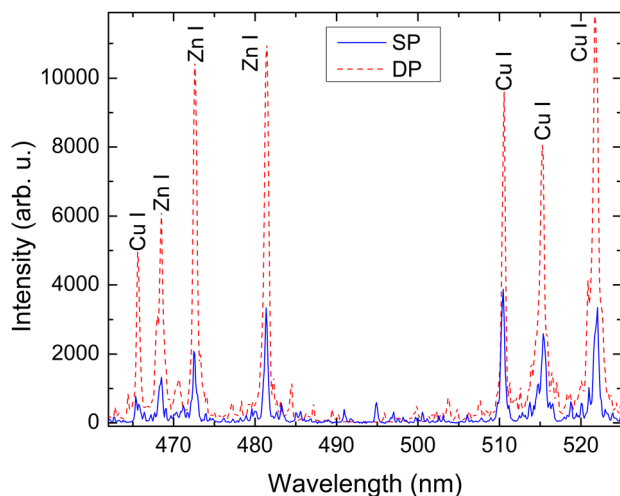


FIG. 2. Typical spectra from fs single plasma and double plasma. The laser fluence used for the single pulse was  $12.72 \text{ J/cm}^2$  (laser energy  $\sim 1 \text{ mJ}$ ) which was equivalent to the sum of the pre-pulse and the delayed pulse energy fluences in DP experiments. An inter-pulse delay of 20 ps was used for recording DP LIBS spectrum.

elements in the sample as well as the use of non-gated detectors for analysis. Interestingly, fs plasma is devoid of any ionic species emission and is dominated by atomic emission. The difference in spectral features can again be attributed to laser ablation mechanisms in fs LA, which produces a plume dominated by mostly neutral species resulting from thermal vaporization. Thermal vaporization produces mostly atomic plume, as temperatures of the emitted species are near the vaporization point of the bulk and such species were far enough below the surface that ionization by the laser pulse is minimized.<sup>5</sup>

The signal enhancements in DP-LIBS scheme are depended strongly on inter-pulse delay ( $\tau_{\text{delay}}$ ). Previous studies showed that a typical inter-pulse delay of  $\sim 1 \mu\text{s}$  was appropriate for ns DP-LIBS.<sup>14,18</sup> The estimated signal enhancements for Zn I at 481.05 nm and Cu I at 510.55 nm are given in Figure 3 for  $\tau_{\text{delay}}$  up to 50 ps. The signal enhancements given in the plot correspond to normalized DP signal intensity with respect to signal intensity obtained from SP experiments ( $I_{\text{DP}}/I_{\text{SP}}$ ). For direct comparison, single pulse energy of 1 mJ was used which was equivalent to sum of the energy for pre- and delayed pulses. Signal enhancement curve for both Cu I and Zn I emission lines approximately followed similar trajectory with respect to  $\tau_{\text{delay}}$ , though with differences in absolute enhancement. The signal enhancement plot given in Figure 3 shows an optimum inter-pulse delay  $\sim 20$  ps. At  $\Delta t = 0$ , the expected value of  $I_{\text{DP}}/I_{\text{SP}} \sim 1$  considering the laser energy used for single and dual pulse experiments are similar.

According to Figure 3, the signal enhancement for DP scheme is significant and reaches maximum when the  $\tau_{\text{delay}} \sim 20$  ps. The signal enhancement curve showed a slight reduction when  $\tau_{\text{delay}}$  is increased beyond  $\sim 20$  ps. Even though DP LIBS experiments always provided higher sensitivity, there exists some controversy in explaining the exact mechanisms causing the improved sensitivity which include higher mass ablation, larger plasma volume, reheating of the plume, lowering of laser shielding effect, heating of the target by the first pulse and the reduction in ambient density,

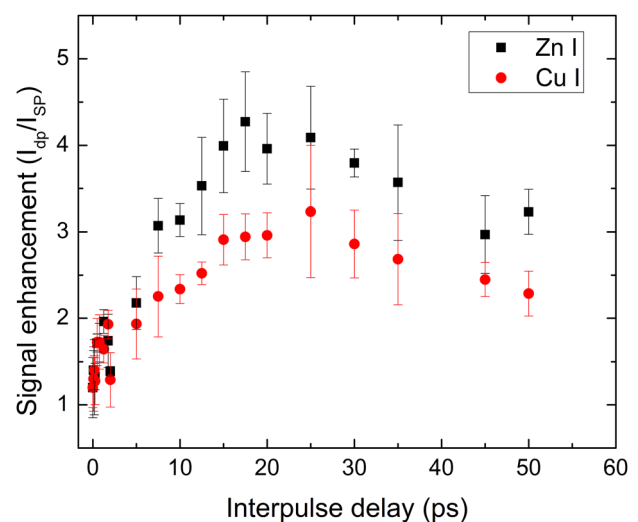


FIG. 3. The signal enhancement recorded for Zn I 481.05 nm and Cu I 510.55 nm lines for DP fs LIBS with respect to single pulse LIBS. For direct comparison a single pulse energy of 1 mJ was used which was equivalent to the sum of the energy for pre and delayed pulses in DP scheme.

rekindling of the plume, or combination of some of the above mechanisms.<sup>14</sup> However, the mechanisms leading to signal enhancement may be different for various experimental configurations as well as laser parameters. For ns LIBS, the critical density  $n_c$  plays an important role in governing laser-target and laser plasma coupling which is strongly dependent on excitation laser wavelength  $\lambda$  ( $n_c = 10^{21}/\lambda^2$ ). For example, the reheating mechanism is prevalent for DP scheme employing a combination of NIR-IR laser (e.g., 1.06  $\mu\text{m}$ -10.6  $\mu\text{m}$ ).<sup>15</sup> Since the typical optimal  $\tau_{\text{delay}}$  observed for ns DP LIBS experiments ( $\sim 0.5 \mu\text{s} - 2 \mu\text{s}$ ) significantly higher compared to DP-LIBS employing fs lasers, which is  $\sim 20$  ps, some of these processes can easily be ruled out in the present experiments. In ns LIBS, plasma heating is predominant even with single pulse experiments because of long duration of the laser pulse compared to plasma formation time. In ULIBS, plasma formation happens at later times ( $\sim$  a few ps) compared to excitation laser pulse duration. The signal enhancements noticed in the experiment are in the range 3-4 $\times$ . Pinon *et al.*<sup>19</sup> reported significantly higher (5-9 $\times$ ) signal enhancement during their DP experiments using similar experimental scheme compared to the present work using 248 nm, 450 fs laser excitation. The higher signal enhancement factor observed could be due to differences in experimental conditions (laser fluence, wavelength, pulse width, and spot size) compared to the present work. They also noticed sudden signal enhancement in the early times ( $< 20$  ps) followed by a plateau region.<sup>19</sup>

The excitation temperature ( $T_{\text{exc}}$ ) of the plume are estimated using Boltzmann plot method employing Cu I lines<sup>6</sup> and the results are shown in Figure 4 for various  $\tau_{\text{delay}}$ . The intensity of Cu I lines at 427.51, 465.11, 510.55, 515.32, and 521.82 nm were used for generating Boltzmann plot. The temperature plot showed approximately stagnant temperature values until  $\sim 5$  ps and a gradual increase in excitation temperature at later times. The estimated temperature for single pulse plasma is  $\sim 9800 \pm 300$  K which is approximately similar to a DP scenario at short inter-pulse delays ( $\tau_{\text{delay}} < 5$  ps). A comparison between signal enhancement as well as excitation temperature curves with respect to the inter-

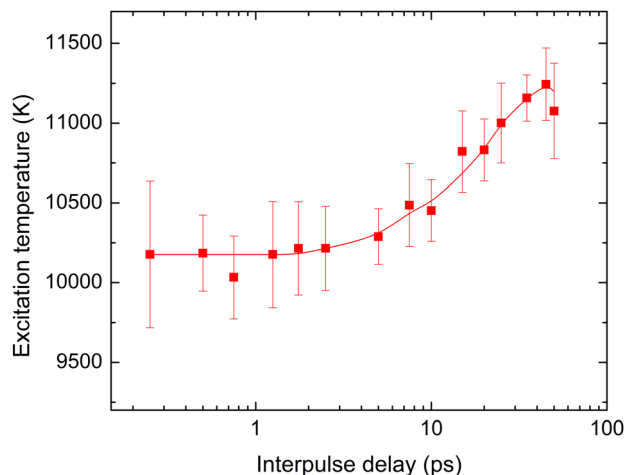


FIG. 4. The excitation temperature of the fs DP plasma plume estimated using the Boltzmann method for various inter-pulse delay. The estimated excitation temperature for single fs pulse LIBS (or ULIBS) was  $9800 \pm 300$  K.

pulse delays indicate that reheating of the pre-formed plume may play an important role in the DP-ULIBS scheme.

The signal enhancement with respect to inter-pulse delay showed differences in maximum enhancement for selected Cu and Zn lines (Figure 3). Though both lines showed maximum enhancement  $\sim 20$  ps, the respective signal enhancements were  $\sim 3$  and  $\sim 4$  for Cu I and Zn I lines, respectively. This implies that the sensitivity in DP-ULIBS could be related to the upper excitation level of the transitions of atomic lines (Cu I 30 783.68  $\text{cm}^{-1}$  and Zn I 53 672.28  $\text{cm}^{-1}$ ). We examined the signal enhancement factor for various Cu and Zn emission transitions with differing upper energy levels and the results are shown in Figure 5 for different inter-pulse delays. This figure clearly shows that the signal enhancement factor is strongly dependent on the upper energy levels of emitting lines and enhancement is found to be higher for lines originating from higher energy levels. This clearly highlights that the reheating mechanism is responsible for signal enhancement in DP-ULIBS, which is consistent with the excitation temperature estimate.

We also evaluated the dependence of laser energy on single and dual pulse integrated signal intensity and results are given in Figure 6 for Cu I transition at 510.55 nm. The DP measurements were performed at an inter-pulse delay of 20 ps. The signal intensity in both SP and DP cases increased steeply with respect to laser energy and it is very clear from the figure that the signal enhancement in the DP is significantly higher compared to single pulse under similar laser fluence conditions. It also shows the enhancement factor is increased for higher energies, which implies that more reheating by the delayed pulse of the ablation plume materials generated by the first pulse. Similar intensity tendency with laser fluence is also reported in Ref. 16 and explained due to hotter and longer-lived plasma for the signal enhancement of DP LIBS in comparison with single pulse configuration.

The signal enhancement factors as well as excitation temperature curves showed a rapid increase when the  $\tau_{\text{delay}} > 5$  ps. When the  $\tau_{\text{delay}} < 5$  ps, the enhancement factor is

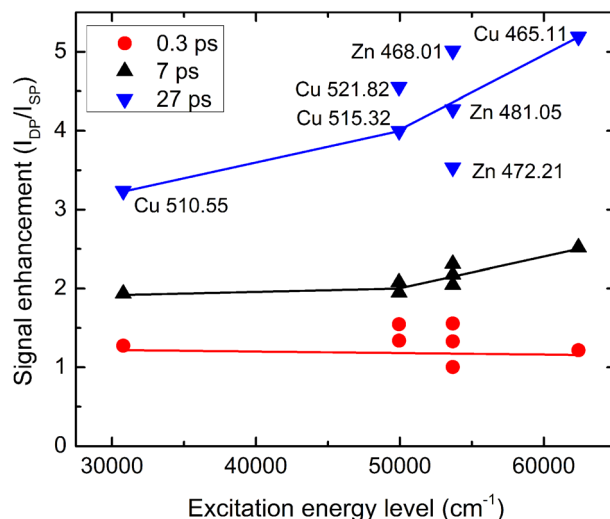


FIG. 5. Signal enhancement for various emission lines in the DP plasma with respect to their upper excitation energy levels for three inter-pulse delays. A 0.5 mJ laser energy was used for both beams.

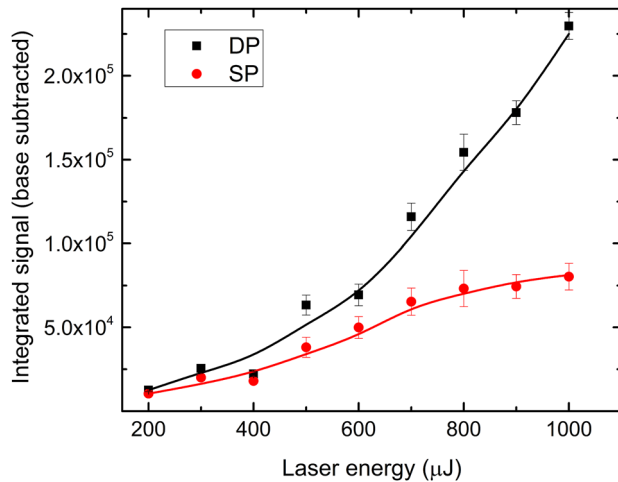


FIG. 6. Emission intensity of Cu I line at 510.55 nm as a function of laser pulse energy for SP and DP ULIBS schemes. An inter-pulse delay of 20 ps was used for DP measurements.

negligible with the excitation temperature was similar to single pulse LIBS. Recent experiments<sup>20</sup> and simulations<sup>21</sup> of DP fs LA using metal targets showed monotonic decrease in ablation crater depth as well as reduction in nanoparticle generation<sup>17,20</sup> when  $\tau_{\text{delay}}$  is greater than the electron-ion relaxation times  $\tau_{\text{ei}}$ . This effect was noticed both in air<sup>22</sup> as well as in vacuum<sup>20</sup> and explained as the suppression of the rarefaction wave caused by heating of the first layer of the ablated material located in front of the target rather than coupling of the second pulse with the target material leading to reduction in ablation efficiency.<sup>21</sup> Since the laser pulse duration used in the present experiment ( $t_p \sim 100$  fs) is significantly shorter than the characteristic relaxation times ( $\tau_{\text{ei}}$ ), electron heat conduction time ( $t_{\text{heat}}$ ), and thus also shorter than the plasma generation and hydrodynamics expansion time; ( $\tau_{\text{ei}} \sim t_{\text{heat}} \gg t_p$ ) all of which typically occur on the order of several picoseconds after laser absorption. Since  $\tau_{\text{ei}}$  scales with atomic mass number of the ion<sup>23</sup> and considering  $\tau_{\text{ei}} \sim 7$  ps for Cu,<sup>24</sup> the material ablation in the DP case will be similar to the SP until  $\tau_{\text{delay}} \sim \tau_{\text{ei}}$ . The estimated excitation temperature is also agreeing well with this argument where the temperature is found to be approximately constant until the  $\tau_{\text{delay}}$  reaches  $\sim \tau_{\text{ei}}$  and increases when  $\tau_{\text{delay}} > 5$  ps which corresponds to characteristic electron-ion relaxation time of Cu.

In conclusion, we investigated the fs- DP-LIBS and noticed significant signal enhancement with respect to single pulse LIBS. The signal enhancement greatly depended on inter-pulse delay and maximum enhancement was observed  $\sim 20$  ps for the system studied. The signal enhancement is found to be greater for lines having higher excitation energy. The excitation temperature analysis showed steeper temperature increase when the inter-pulse delay is greater than that

of electron-ion relaxation time. Based on excitation temperature curve as well as the enhancement factor with respect to laser energy, we concluded that the reheating by the delayed pulse of the ablation plume generated by the first pulse is the main mechanism for improved signal intensity in DP ULIBS. This is also supported by the fact that higher signal enhancement observed for the lines originating from higher excitation energy. Compared to ns-DP-LIBS, where typically two lasers are used for DP geometry, the collinear fs-DP-LIBS arrangement employing a Michelson interferometer is simpler and easy to adapt.

This work was partially supported by the US DOE National Nuclear Security Administration under Award No. DE-NA0001174.

- <sup>1</sup>M. Sabsabi, in *Laser-Induced Breakdown Spectroscopy*, edited by J. P. Singh and S. N. Thakur (Elsevier, Amsterdam, 2007).
- <sup>2</sup>M. R. Leahy-Hoppa, J. Miragliotta, R. Oslander, J. Burnett, Y. Dikmelik, C. McEnnis, and J. B. Spicer, *Sensors (Basel)* **10**, 4342 (2010).
- <sup>3</sup>V. Zorba, J. Syzdek, X. L. Mao, R. E. Russo, and R. Kostecki, *Appl. Phys. Lett.* **100**, 234101 (2012).
- <sup>4</sup>E. L. Gurevich and R. Hergenroder, *Appl. Spectrosc.* **61**, 233A (2007).
- <sup>5</sup>R. Stoian, D. Ashkenasi, A. Rosenfeld, and E. E. B. Campbell, *Phys. Rev. B* **62**, 13167 (2000).
- <sup>6</sup>B. Verhoff, S. S. Harilal, J. Freeman, P. K. Diwakar, and A. Hassanein, *J. Appl. Phys.* **112**, 093303 (2012).
- <sup>7</sup>M. Baudelet, L. Guyon, J. Yu, J. P. Wolf, T. Amodeo, E. Frejafon, and P. Laloi, *Appl. Phys. Lett.* **88**, 063901 (2006).
- <sup>8</sup>M. Kotzagianni and S. Couris, *Appl. Phys. Lett.* **100**, 264104 (2012).
- <sup>9</sup>K. F. Al-Shboul, S. S. Harilal, and A. Hassanein, *Appl. Phys. Lett.* **100**, 221106 (2012).
- <sup>10</sup>K. Stelmaszczyk, P. Rohwetter, G. Mejean, J. Yu, E. Salmon, J. Kasparian, R. Ackermann, J. P. Wolf, and L. Woste, *Appl. Phys. Lett.* **85**, 3977 (2004).
- <sup>11</sup>D. W. Hahn and N. Omenetto, *Appl. Spectrosc.* **66**, 347 (2012).
- <sup>12</sup>K. Hatanaka, H. Ono, and H. Fukumura, *Appl. Phys. Lett.* **93**, 064103 (2008).
- <sup>13</sup>J. R. Freeman, S. S. Harilal, and A. Hassanein, *J. Appl. Phys.* **110**, 083303 (2011).
- <sup>14</sup>V. I. Babushok, F. C. DeLucia, Jr., J. L. Gottfried, C. A. Munson, and A. W. Miziolek, *Spectrochim. Acta, Part B* **61**, 999 (2006).
- <sup>15</sup>R. W. Coons, S. S. Harilal, S. M. Hassan, and A. Hassanein, *Appl. Phys. B* **107**, 873 (2012).
- <sup>16</sup>V. Pinon and D. Anglos, *Spectrochim. Acta, Part B* **64**, 950 (2009).
- <sup>17</sup>S. Amoroso, R. Bruzzese, and X. Wang, *Appl. Phys. Lett.* **95**, 251501 (2009).
- <sup>18</sup>P. K. Diwakar, S. S. Harilal, J. R. Freeman, and A. Hassanein, *Spectrochim. Acta Part B* (2013) (published online).
- <sup>19</sup>V. Pinon, C. Fotakis, G. Nicolas, and D. Anglos, *Spectrochim. Acta, Part B* **63**, 1006 (2008).
- <sup>20</sup>S. Noel and J. Hermann, *Appl. Phys. Lett.* **94**, 053120 (2009).
- <sup>21</sup>M. E. Povarnitsyn, T. E. Itina, K. V. Khishchenko, and P. R. Levashov, *Phys. Rev. Lett.* **103**, 195002 (2009).
- <sup>22</sup>A. Semerok and C. Dutouquet, *Thin Solid Films* **453**, 501 (2004).
- <sup>23</sup>Y. B. Zeldovich and Y. P. Raizer, *Physics of Shock Waves and High-Temperature Hydrodynamic Phenomena* (Dover Publications, Inc., New York, 2002).
- <sup>24</sup>C. Schafer, H. M. Urbassek, and L. V. Zhigilei, *Phys. Rev. B* **66**, 115404 (2002).